Supporting Information for ***Journal of Materials Chemistry A***

MXene-derived TiO_2/reduced graphene oxide composite with an enhanced capacitive capacity for Li and K ion batteries

Yongzheng Fang,[a] Rong Hu, [a] Boya Liu, [a] Yingying Zhang, [a] Kai Zhu,*[a] Jun Yan, [a] Ke Ye, [a] Kui Cheng, [a] Guiling Wang, [a] and Dianxue Cao* [a]

[a] *Key Laboratory of Superlight Materials and Surface Technology, Ministry of Education, College of Material Science and Chemical Engineering, Harbin Engineering University, Harbin 150001, China*

Table S1. Determination of the size in TiO_2/RGO.

Sample	Index	2θ (degree)	β (degree)	Diameter(nm)
TiO_2/RGO	(101)	25.303	0.49	16.44

Calculation method: the Scherrer equation [1]:

$$\text{Diameter} = 0.89*\lambda/(\beta*\cos\theta) \quad [1]$$

The λ is the wavelength of the X-ray (0.15418 nm) and β is the full width at half maximum of the diffraction peak.

Table S2. The cycling performance at low and high current density contrast with literature.

Refer	Current density (mA/g)	Cycles and retention	Current density (mA/g)	Cycles and retention
The work	**200**	**200, 78%**	**1000**	**1000, 85%**
1	140	150,83%	280	500,75%
2	100	300,68%	100	1000,65%
3	200	200, 90%	1000	1000, 70%
4	200	200, 100%	1000	600, 100%
5	100	100, 94%	500	500, 80%
6	200	100, 62.5%	--	--
7	55.8	100, 90%	558	500, 94.6%
8	200	500, 60%	--	--
9	500	200, 78%	--	--
10	50	100, 96%	--	--
11	400	400,72.8%	--	--

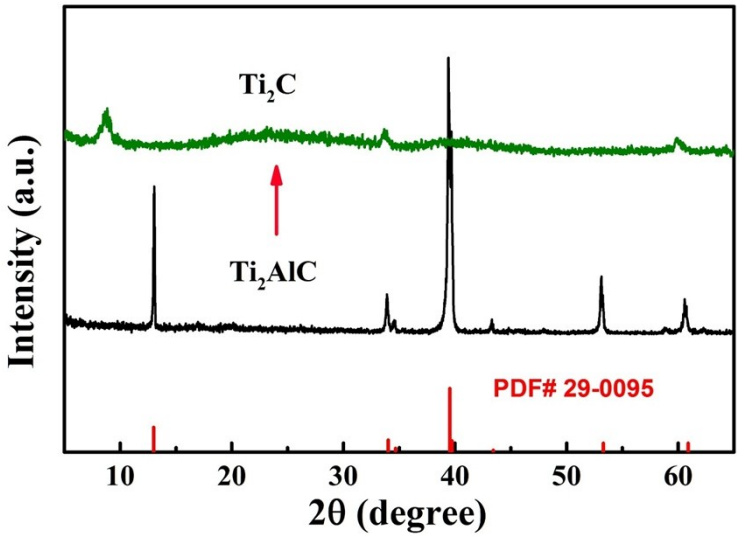

Figure S1. XRD of the Ti_2AlC and the Ti_2C.

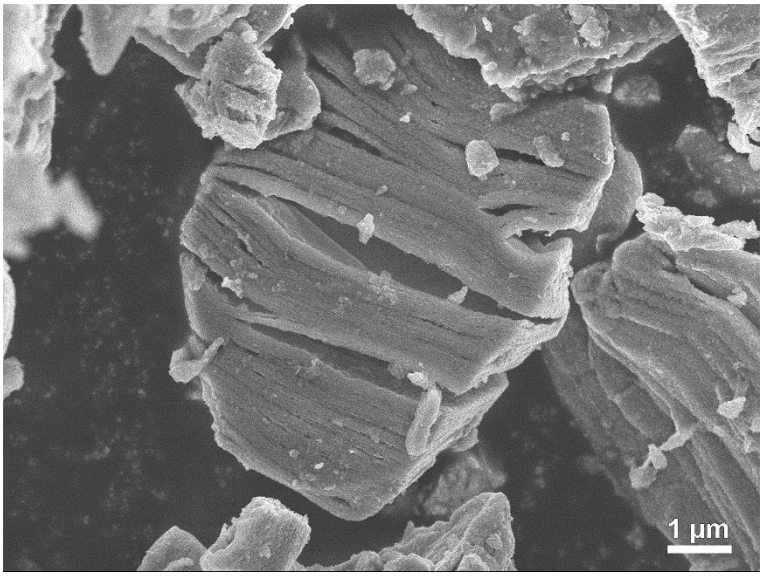

Figure S2. SEM of the multilayer Ti_2C.

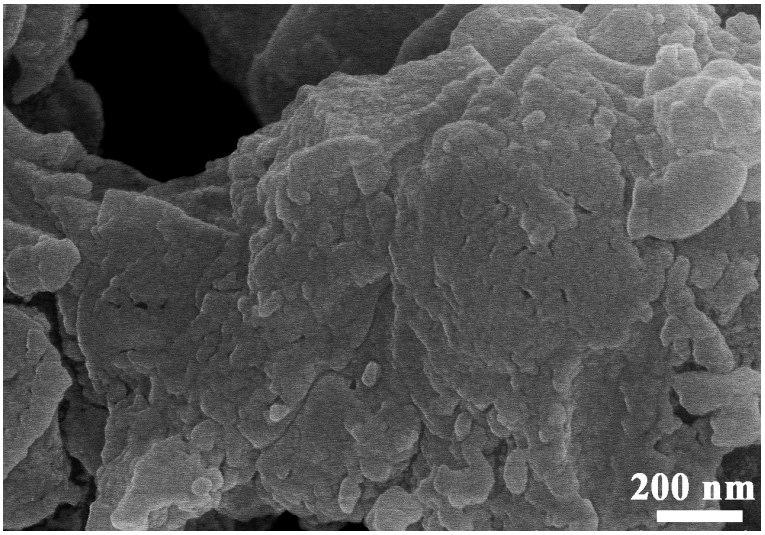

Figure S3. SEM of the amorphous Ti-based intermediates.

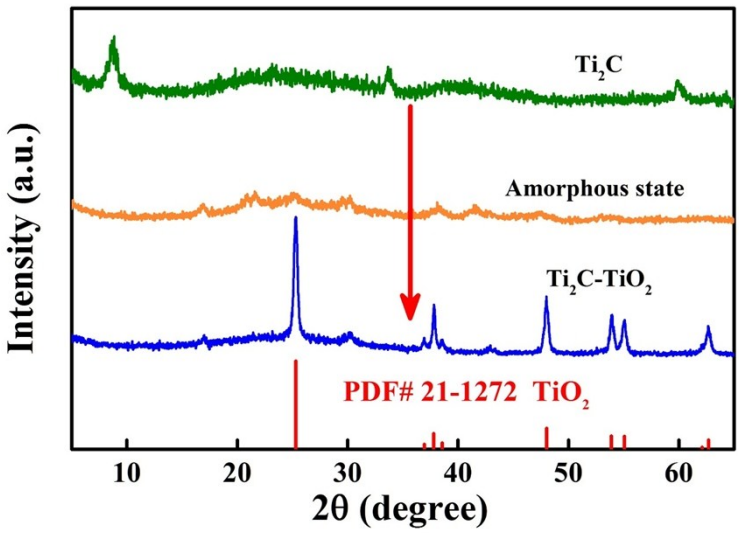

Figure S4. XRD of the change process from the Ti_2C to amorphous state to the Ti_2C - derived TiO_2.

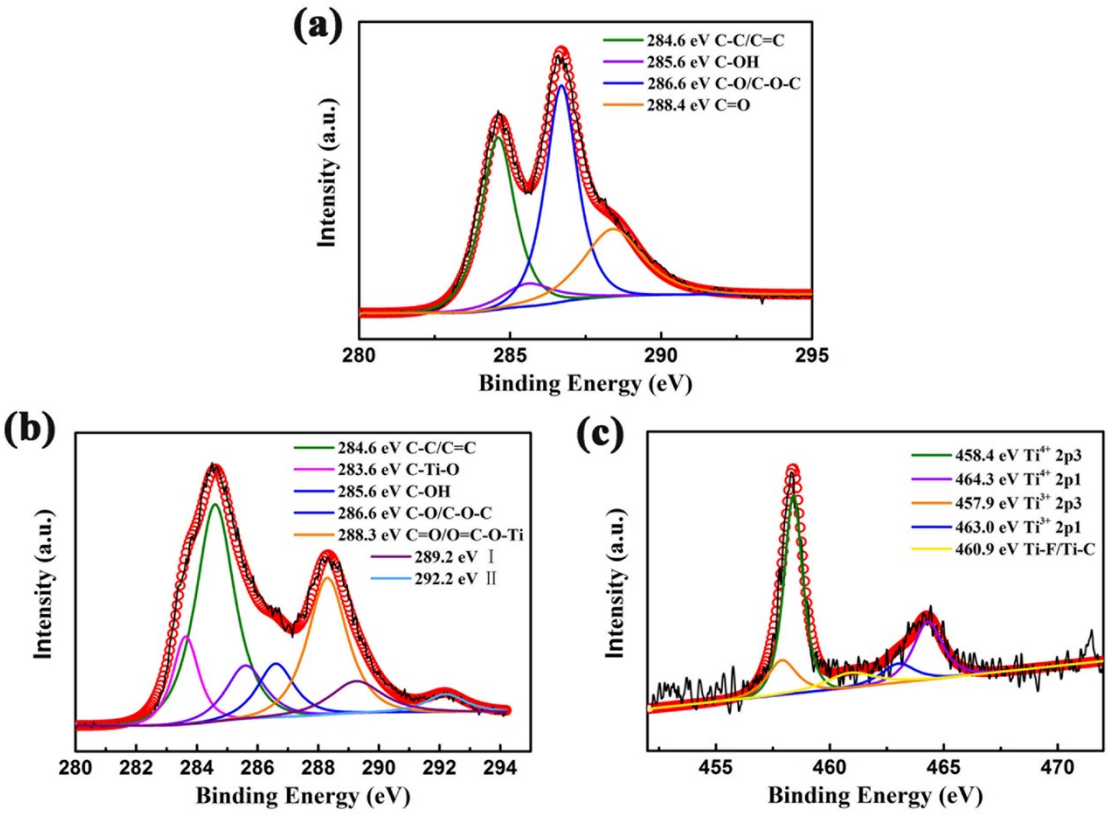

Figure S5. XPS images of GO and TiO_2/RGO composite. (a) C1s image of GO. (b) C1s image of TiO_2/RGO. (c) Ti2p of TiO_2/RGO.

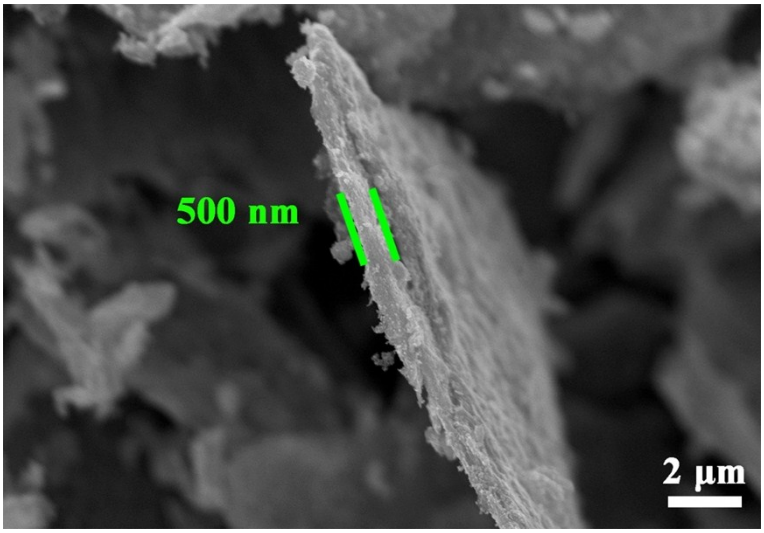

Figure S6. Cross-section SEM of the sandwich sheet-like TiO_2/RGO. The TiO_2/RGO sheets show a tight and unstacked structure, which indicates a good interaction between TiO_2 and RGO. The thickness of TiO_2/RGO sheets is about 500 nm.

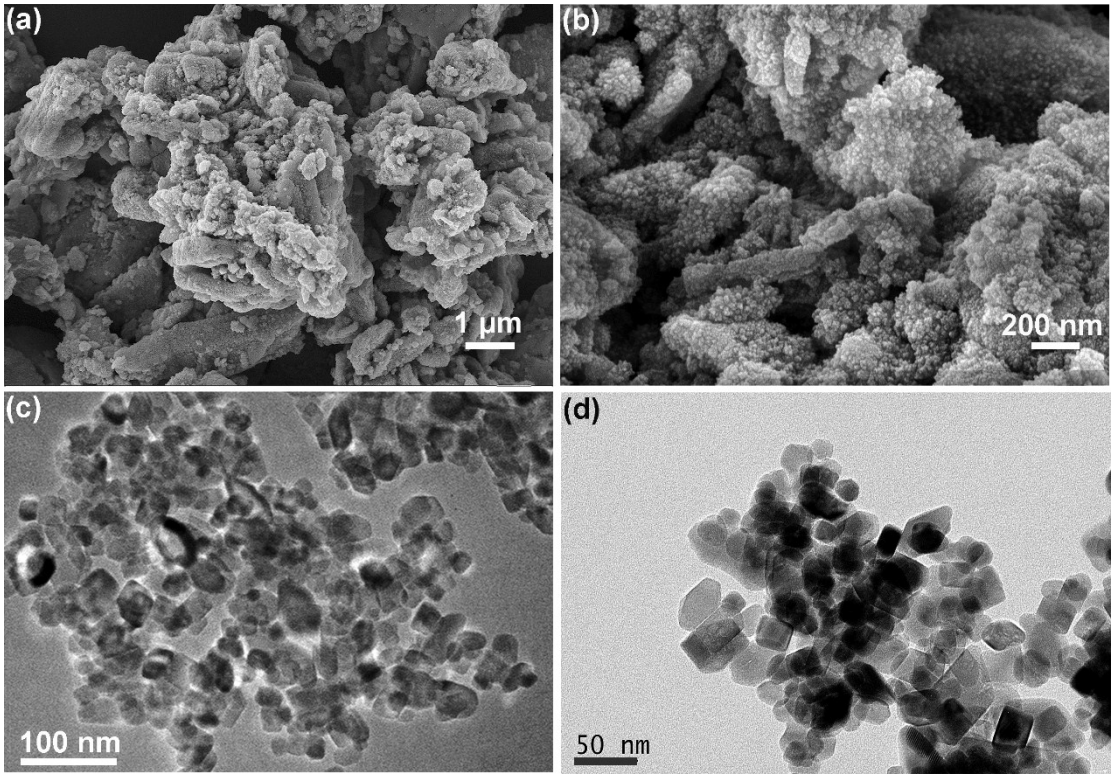

Figure S7. The microtopography of Ti_2C-TiO_2. (a), (b) SEM images. (c), (d) TEM images.

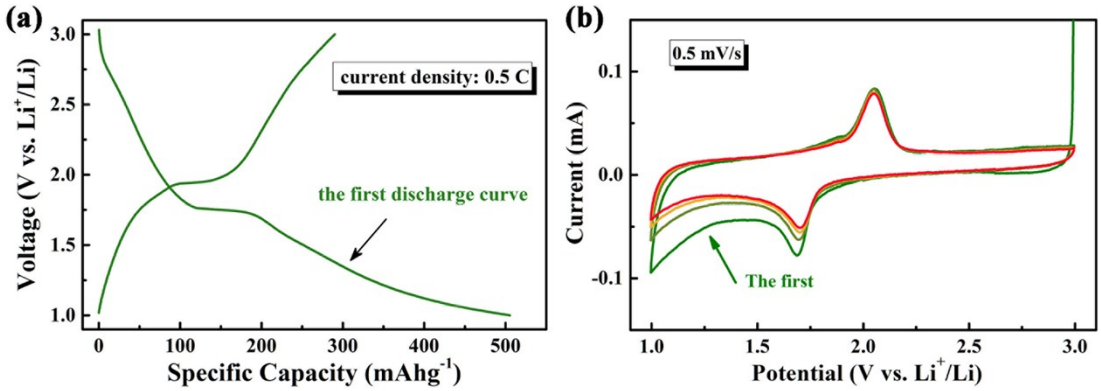

Figure S8. (a) the charge-discharge curves in the first cycle; (b) the initial CV curves. of TiO_2/RGO.

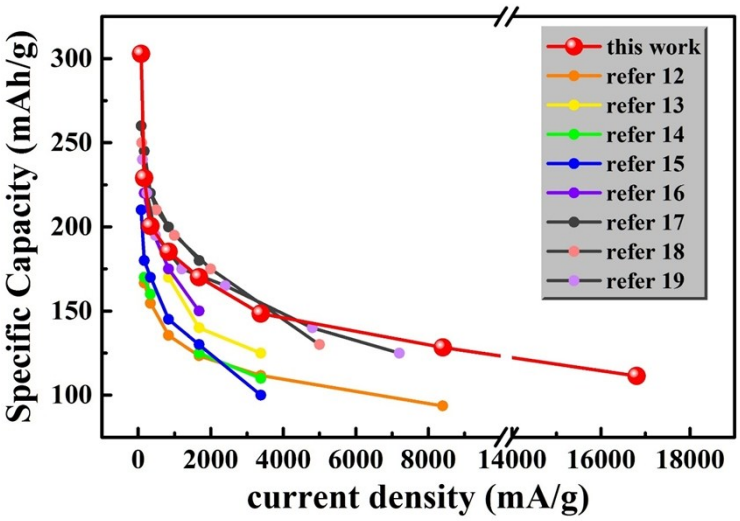

Figure S9. The rate performance comparison of LIBs between TiO_2/RGO and other TiO_2 anode.

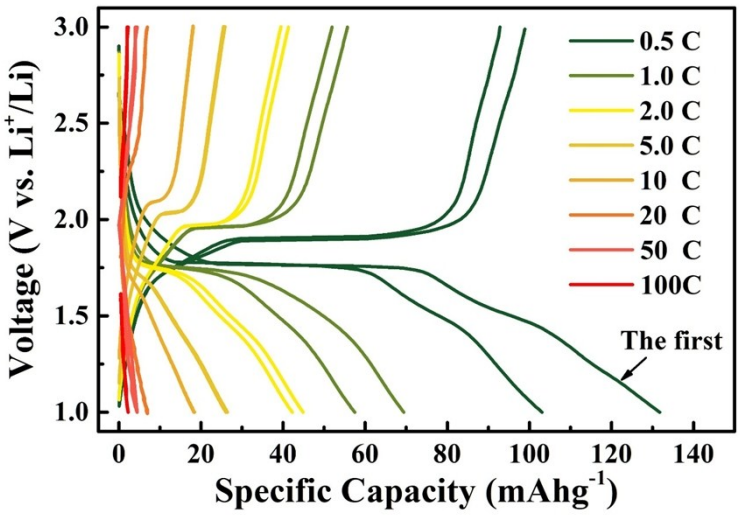

Figure S10. The charge-discharge curves of Ti_2C-TiO_2 at different current density

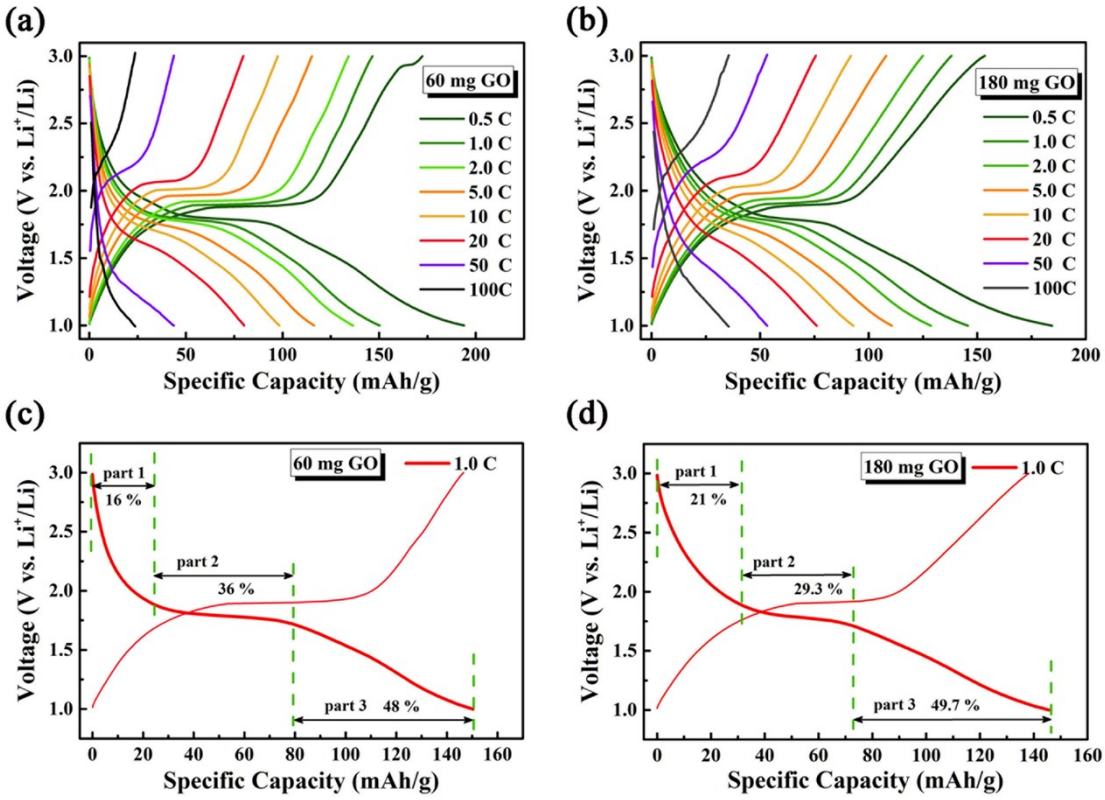

Figure S11. The charge-discharge curves of (a) TiO_2/RGO-60 and (b) TiO_2/RGO-180 at different current density; charge-discharge curves of (c) TiO_2/RGO-60 and (d) TiO_2/RGO-180 at 1.0 C.

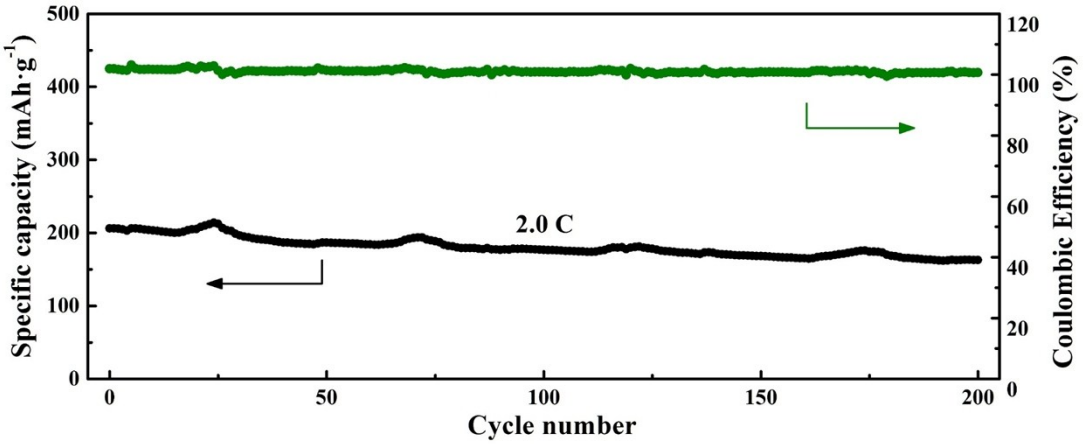

Figure S12. The 200 cycles performance of TiO_2/RGO at 2.0 C.

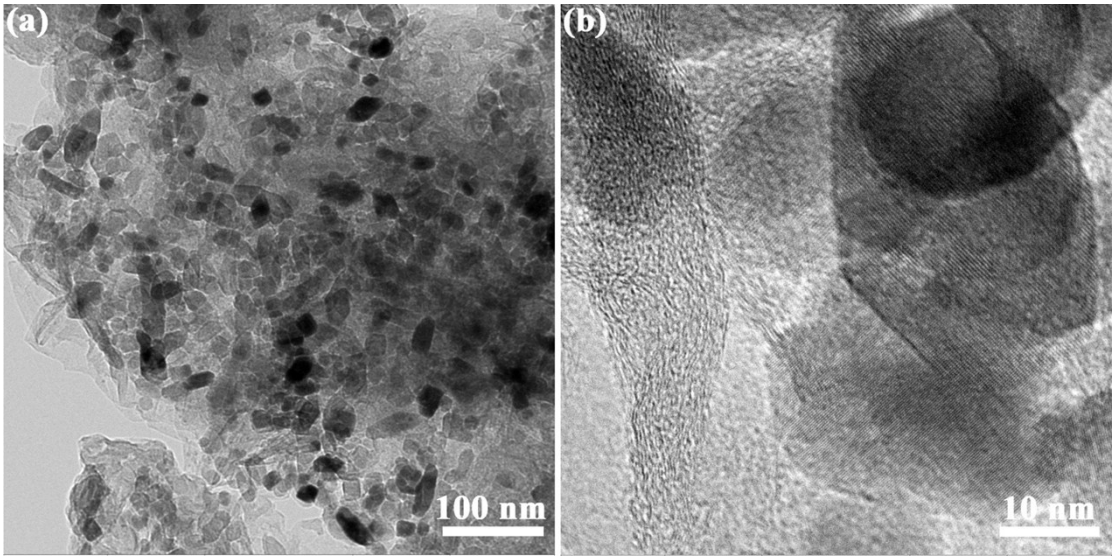

Figure S13. TEM image of TiO_2/RGO after cycling.

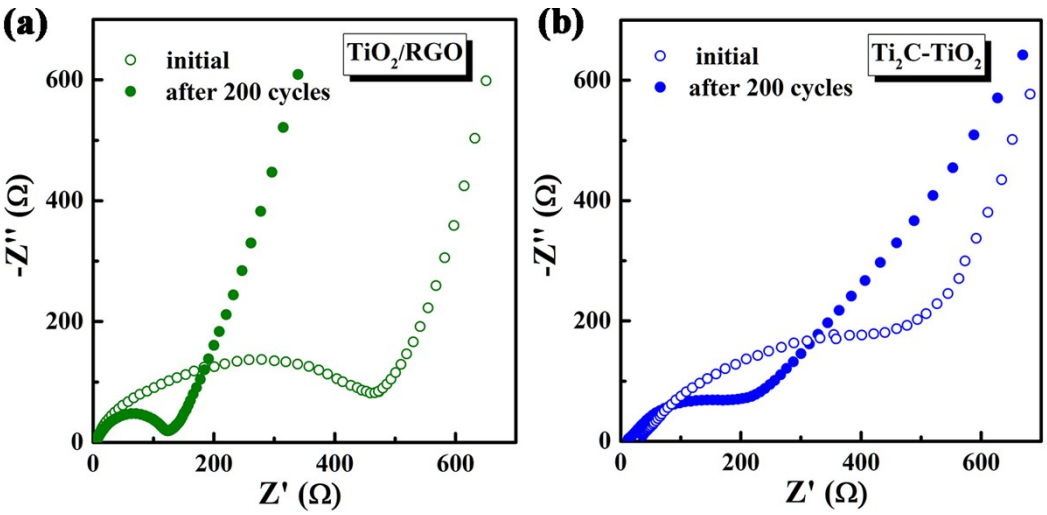

Figure S14. EIS curves at initial and after 200 cycles. (a) TiO_2/RGO (b) Ti_2C-TiO_2.

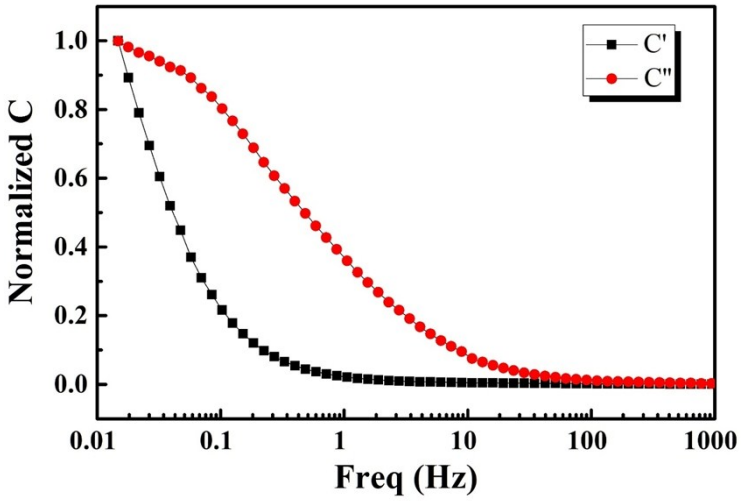

Figure S15. Normalized real and imaginary capacitances of the Ti_2C-TiO_2.

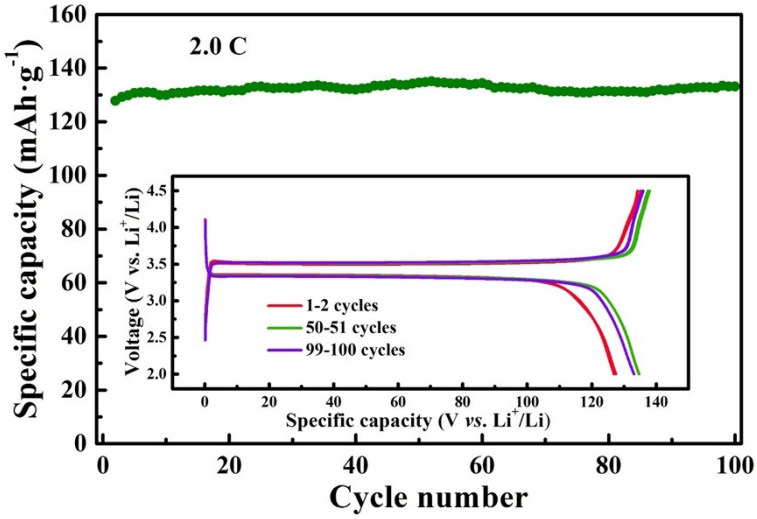

Figure S16. The cycle performance of the $LiFePO_4$. The charge-discharge curves in the illustration.

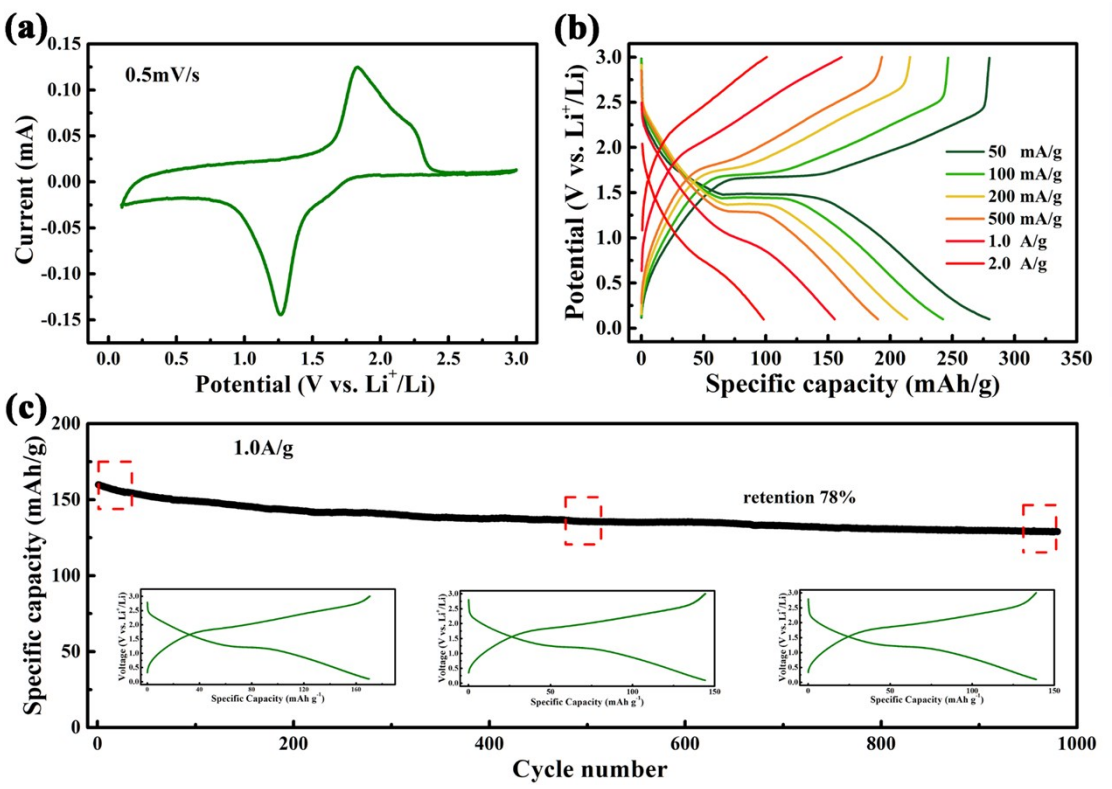

Figure S17. The performance of full cell with $LiFePO_4$ as cathode and TiO_2/RGO as anode. (a) the CV curve at 0.5 mV/s. (b) The charge-discharge curves at different current density. (c) The 1000 cycles performance at 1.0 A/g, the capacity retention was 78%.

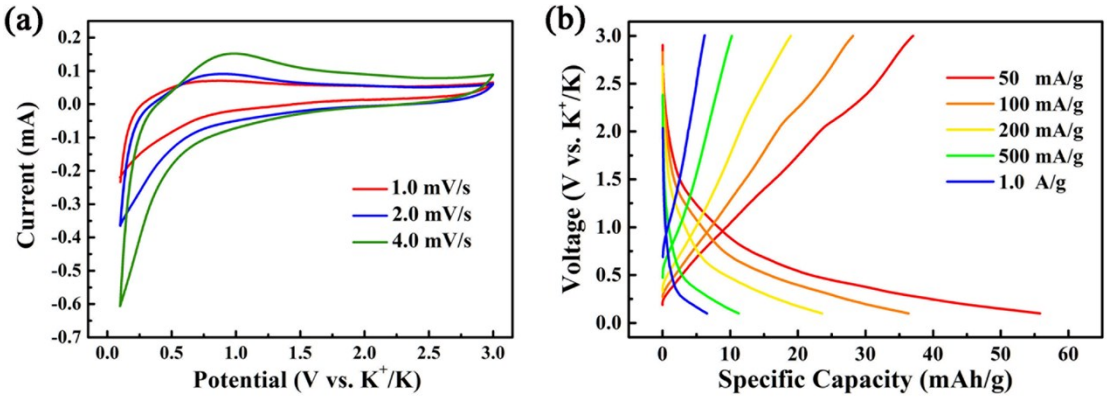

Figure S18. The performance of Ti_2C-TiO_2. (a) The CV curves at different scan rates.

(b) The charge-discharge curves at different current density.

References

1. D. S. Bin, X. J. Lin, Y. G. Sun, Y. S. Xu, K. Zhang, A. M. Cao and L. J. Wan, 2018.
2. J. Y. Hwang, J. Kim, T. Y. Yu, S. T. Myung and Y. K. Sun, *Energy & Environmental Science*, 2018.
3. W. Wang, J. H. Zhou, Z. P. Wang, L. Y. Zhao, P. H. Li, Y. Yang, C. Yang, H. X. Huang and S. J. Guo, *Advanced Energy Materials*, 2018, **8**.
4. C. Li, X. Hu and B. Hu, *Electrochimica Acta*, 2017, **253**.
5. X. P. Wang, K. Han, D. D. Qin, Q. Li, C. Y. Wang, C. J. Niu and L. Q. Mai, *Nanoscale*, 2017, **9**, 18216-18222.
6. Z. Tai, Q. Zhang, Y. Liu, H. Liu and S. Dou, *Carbon*, 2017, **123**.
7. R. Hao, H. Lan, C. Kuang, H. Wang and L. Guo, *Carbon*, 2018, **128**.
8. P. C. Lian, Y. F. Dong, Z. S. Wu, S. H. Zheng, X. H. Wang, S. Wang, C. L. Sun, J. Q. Qin, X. Y. Shi and X. H. Bao, *Nano Energy*, 2017, **40**, 1-8.
9. J. Z, Z. S, X. Z, Z. Q, Q. Y and Q. Y, *Acs Appl Mater Interfaces*, 2016, **8**, 20682-20690.
10. K. Share, A. P. Cohn, R. Carter, B. Rogers and C. L. Pint, *Acs Nano*, 2016, **10**.
11. N. Li, F. Zhang and Y. B. Tang, *Journal of Materials Chemistry A*, 2018, **6**, 17889-17895.
12. J. Chen, W. Song, H. Hou, Z. Yan, M. Jing, X. Jia and X. Ji, *Advanced Functional Materials*, 2016, **25**, 6793-6801.
13. S. X. Yu, L. W. Yang, Y. Tian, P. Yang, F. Jiang, S. W. Hu, X. L. Wei and J. X. Zhong, *Journal of Materials Chemistry A*, 2013, **1**, 12750-12758.
14. W. Donghai, C. Daiwon, L. Juan, Y. Zhenguo, N. Zimin, K. Rong, H. Dehong, W. Chongmin, L. V. Saraf and Z. Jiguang, *Acs Nano*, 2009, **3**, 907-914.
15. Y. Cai, H. E. Wang, S. Z. Huang, M. F. Yuen, H. H. Cai, C. Wang, Y. Yu, Y. Li, W. J. Zhang and B. L. Su, *Electrochimica Acta*, 2016, **210**, 206-214.
16. J. Liu, Z. Ping, T. Han, J. Huang, J. Liu, J. Li and P. V. Braun, *Materials Letters*, 2018, **219**, S0167577X18302428.
17. X. Li, G. Wu, L. Xin, L. Wei and M. Li, *Nano Energy*, 2017, **31**, 1-8.
18. D. H. Lee, B. H. Lee, A. K. Sinha, J. H. Park, M. S. Kim, J. Park, H. Shin, K. S. Lee, Y. E. Sung and T. Hyeon, *Journal of the American Chemical Society*.
19. Y. Cheng, C. Zheng, H. Wu, M. Zhu and Y. Lu, *Advanced Functional Materials*, 2016, **26**, 1487-1487.